Earth and Planetary Science Letters 393 (2014) 26–30

Contents lists available at ScienceDirect

Earth and Planetary Science Letters

www.elsevier.com/locate/epsl

Spontaneous ice-front retreat caused by disintegration of adjacent ice shelf in Antarctica

Torsten Albrecht [a,b,*], Anders Levermann [a,b]

[a] Earth System Analysis, Potsdam Institute for Climate Impact Research, Potsdam, Germany
[b] Institute of Physics and Astronomy, University of Potsdam, Potsdam, Germany

ARTICLE INFO

Article history:
Received 2 October 2013
Received in revised form 9 February 2014
Accepted 13 February 2014
Available online xxxx
Editor: J. Lynch-Stieglitz

Keywords:
Antarctica
Larsen Ice Shelf
glaciology
numerical ice modeling
sea level
iceberg calving

ABSTRACT

Antarctic ice-discharge constitutes the largest uncertainty in future sea-level projections. Floating ice shelves, fringing most of Antarctica, exert retentive forces onto the ice flow. While abrupt ice–shelf retreat has been observed, it is generally considered a localized phenomenon. Here we show that the disintegration of an ice shelf may induce the spontaneous retreat of its neighbor. As an example, we reproduce the spontaneous but gradual retreat of the Larsen B ice front as observed after the disintegration of the adjacent Larsen A ice shelf. We show that the Larsen A collapse yields a change in spreading rate in Larsen B via their connecting ice channels and thereby causes a retreat of the ice front to its observed position of the year 2000, prior to its collapse. This mechanism might be particularly relevant for the role of East Antarctica and the Antarctic Peninsula in future sea level.

1. Introduction

Significant progress has been made in understanding past sea-level changes (Payne et al., 2007; Gregory et al., 2012; Church et al., 2011; Lorbacher et al., 2010; Cazenave and Llovel, 2010; Price et al., 2011; Stammer et al., 2013; Levermann et al., 2013). When projecting future sea-level rise an additional difficulty arises. While most of the observed sea-level change was due to the thermal expansion of the ocean and ice loss from mountain glaciers, the contribution of the great ice-sheets on Greenland and Antarctica has been increasing over the last two decades (Van den Broeke et al., 2011; Shepherd et al., 2012; Rignot et al., 2011). As a consequence, observation-driven semi-empirical models still underestimate the observed sea-level rise of that period (Rahmstorf et al., 2007, 2012) and confidence in future projections decreases with the prospect of an increasing role of the ice-sheets. The part of the ice-sheet contribution that can be modeled with some accuracy using process-based models is that from their surface mass balance (Fettweis et al., 2011, 2013; Ettema et al., 2010; Ligtenberg et al., 2013). In contrast, the dynamic solid-ice discharge is difficult to model accurately because several of the physical processes controlling this discharge are difficult to constrain through direct observation. While the ice discharge from Greenland is topographically constrained (Price et al., 2011; Pfeffer et al., 2008), the largest uncertainty for the future resides with the ice loss from Antarctica (Solomon, 2007; Bamber and Aspinall, 2013).

Along most of the Antarctic coast the grounded ice flows into floating ice shelves which exert a retentive force onto the grounded ice sheet (Dupont and Alley, 2005, 2006) and thereby hinder dynamic ice discharge from the continent (Rott et al., 2008, 2011, De Angelis and Skvarca, 2003; Rignot et al., 2004; Scambos et al., 2004; Hulbe et al., 2008). The stability of these ice shelves is thus crucial to understand past and future changes in ice-sheet dynamics and Antarctica's future sea-level contribution (Joughin and Alley, 2011). While abrupt ice–shelf retreat has been observed (Rack and Rott, 2004; Cook and Vaughan, 2010; Glasser and Scambos, 2008), it is generally considered to be a self-contained phenomenon (MacAyeal et al., 2003; Doake et al., 1998; Doake, 2001; Vieli et al., 2006).

Here we investigate the consequences of abrupt disintegration of one ice shelf on the subsequent behavior of adjacent ice shelves. We do not address the specific mechanism of the abrupt disintegration of the ice shelf because we focus on the longer-term processes by which the disappearance of one ice shelf is felt by other ice shelves. Along the Antarctic Peninsula and East Antarctica many ice shelves are separated only partially by ice rises. Examples are the Peninsula ice–shelf Larsen D, Wilkins Ice Shelf and George VI as well as the Brunt/Stancomb-Wills, Riiser-Larsenisen, Fimbulisen, Princessa Ragnhild Kyst and Shackleton in East Antarctica. In these

* Corresponding author at: Potsdam Institute for Climate Impact Research (PIK), Earth System Analysis, Potsdam, Germany.
E-mail address: torsten.albrecht@pik-potsdam.de (T. Albrecht).

http://dx.doi.org/10.1016/j.epsl.2014.02.034
0012-821X/

places adjacent ice shelves are interconnected via channels of currently slow-moving floating ice. A series of ice–shelf disintegration events have been observed which is generally attributed to the warming environment in this most northern part of Antarctica.

One prominent example is the collapse of the Larsen A ice shelf in the year 1995 followed immediately by a sequence of small-scale calving events at the neighboring Larsen B ice shelf (Rack and Rott, 2004; Cook and Vaughan, 2010). This spontaneous response in form of a gradual quasi-continuous retreat of the Larsen B ice front continued in the following years until also Larsen B disintegrated almost completely in 2002. The large-scale abrupt disintegration was very likely caused by ocean-melt induced thinning and meltwater-enhanced fracture processes subdividing the ice shelf into an unstable mélange of ice fragments, which capsize and drain into the open ocean (Glasser and Scambos, 2008; MacAyeal et al., 2003). In contrast, the retreat of the Larsen B front between 1995 and 2000 was quasi-continuous and the result of a large number of small-scale calving events. Here we focus on this continuous but spontaneous ice-front retreat and suggest a mechanism by which the disintegration of an ice shelf leads to the ice-front retreat of an adjacent ice shelf.

2. Methods

The mechanism we propose can be understood independently of numerical model results but is illustrated here using simulations with the thermo-mechanically coupled Potsdam Parallel Ice Sheet Model (PISM-PIK) (Winkelmann et al., 2011), which is based on the open-source Parallel Ice Sheet Model (PISM, version "stable-0.2", Bueler and Brown, 2009). Since only floating ice shelves are considered in this study, the full dynamics captured by PISM is not applied: The velocity field is simply computed according to the Shallow Shelf Approximation (SSA) fed by prescribed inflow at the observed grounding line (Le Brocq et al., 2010). Central to this study is the application of the first-order kinematic calving law (Levermann et al., 2012) (denoted *eigencalving* hereafter), which tries to account for large-scale observational constraints (Doake et al., 1998; Doake, 2001; Alley et al., 2008) into a simple relation. *Eigencalving* is regularly applied in dynamic simulations with PISM (Winkelmann et al., 2012) using a sub-grid scheme for ice-front motion (Albrecht et al., 2011). In order to improve the temporal representation of calving we adapt the time-step within PISM-PIK with an extended version of the CFL-criterion (Courant et al., 1967). It is based on the maximum ice speed and on the maximum computed calving rate in each time step; thereby restricting the calving flux to at most one grid-cell at the ice shelf margin in each time step. Simulations use a horizontal resolution of 1 km.

3. Results

3.1. Basic mechanism of communicating ice shelves

The mechanism of the communication of adjacent ice fronts is illustrated in a simplified geometry of two ice shelves confined in rectangular embayments that are connected by an ice channel (Fig. 1) before applying it to more realistic topography. The ice shelves are fed by a constant inflow at the upstream boundary. The mechanism does not depend on the specific distribution of the inflow. We chose a homogeneous inflow along the entire upper boundary of the basins. The position of the freely moving calving front is generally determined by the inflow of ice, the basin geometry and the calving rate. Here, the ice–shelf system is integrated into dynamical equilibrium for constant boundary conditions with a calving rate, C. This calving rate is proportional to the determinant of the horizontal spreading rate tensor (*eigencalving*)

$$C = K_2^{\pm} \cdot \dot{\epsilon}_- \cdot \dot{\epsilon}_+ \quad \text{for } \dot{\epsilon}_{\pm} > 0 \tag{1}$$

where $\dot{\epsilon}_-$ and $\dot{\epsilon}_+$ are the eigenvalues of the horizontal spreading rate tensor and $K_2^{\pm} = 10^8$ ma is a proportionality constant that incorporates all material properties that are relevant for the calving rate. For simplicity and in order to demonstrate the mechanism, $K_2^{\pm}$ is chosen to be constant in this study. Generally it will depend on ice properties such as the fracture density and ice rheology which might change the results quantitatively but not qualitatively. In order to mimic the rapid disintegration of an ice shelf as observed for example for Larsen A, we eliminate the entire ice shelf on the right-hand side within one time step. This somewhat unrealistic instantaneous collapse allows for investigating the immediate effect on the far-field strain-rate distribution within the remaining ice shelf and best reveals the mechanism: While the flow between the two basins was very small when both ice-shelves were intact (Fig. 1b), the void left by the collapsed ice shelf allows for an ice flow between the two basins (Fig. 1d). Due to the non-local nature of the membrane stresses computed within the ice shelf, the shifted boundary affects the spreading rate in the entire remaining ice shelf (Fig. 1a, c). In particular the spreading perpendicular to the main flow direction, as represented by the minor eigenvalue $\dot{\epsilon}_-$, becomes positive in a large region along the ice front. This results in enhanced calving and a spontaneous initiation of ice-front retreat. It has to be noted that the coarse resolution and the fact that the ice material and flow properties are not realistically captured in our model, the temporal evolution of the ice front is not likely to be captured quantitatively. The effect is however qualitatively robust against changes in boundary condition, lateral friction, calving constant $K_2^{\pm}$ and other ice-properties.

3.2. Application to the Larsen Ice Shelf

Analogous to these conceptual computations, we conduct simulations for a realistic geometry and inflow of the Larsen A and B Ice Shelf system (Fig. 2 and animation in SI). The integration of the model after initialization with realistic boundary conditions yields dynamically stable ice-fronts similar to the observed situation up to 1993 (Fig. 2a, b). We then introduce ad hoc rifts along the side margins in the smaller Larsen A ice shelf that subsequently causes the *eigencalving* process to quickly eliminate the ice shelf. This mimics the observed abrupt disintegration of the Larsen A ice shelf in 1995, while we do not advocate that the actual event occurred like this. Triggering the rapid removal of Larsen A ice shelf, however, is a prerequisite for the main process of interest: the subsequent behavior of Larsen B ice shelf in response.

Since Larsens A and B were connected by a channel of slowly moving ice in the region of Seal Nunataks, the flow across this channel enhances and (following the momentum balance) longitudinal stresses are transferred into Larsen B (Fig. 2c, d). During the first five years after the Larsen A collapse, the modeled ice front of Larsen B undergoes a comparably fast quasi-continuous retreat (Fig. 2e, f) according to the same mechanism described for the conceptual geometry. In the following years the Larsen B ice front retreats with slower pace up to the observed position of Larsen B prior to its full collapse (Fig. 2g, h). The time series of the ice-front position (Fig. 3) reveals the immediate initial retreat followed by a more gradual front motion. This retreat of the calving front in the aftermath of a collapse of the neighboring ice shelf is qualitatively robust against changes in parameters also in the observation-based geometry and velocity distribution of the Larsens A and B ice–shelf system. As reported in earlier studies (Rack and Rott, 2004; Cook and Vaughan, 2010; Glasser and Scambos, 2008), the observed disintegration of the remaining Larsen B ice shelf in 2002 was caused by meltwater-enhanced fracture and was not following the mechanism described here. As mentioned for the conceptual

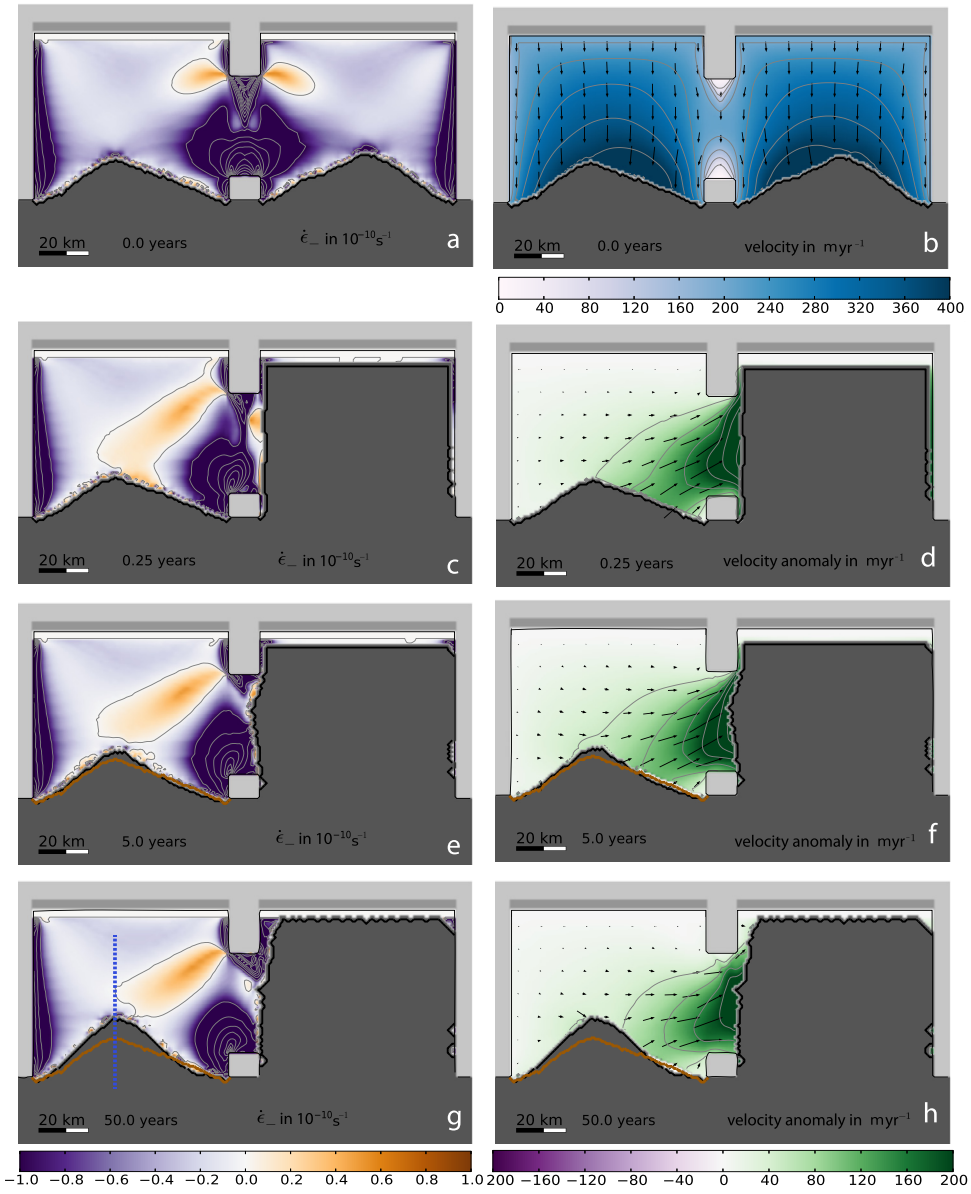

Fig. 1. Mechanism of ice-front retreat (left bay) caused by disintegration of adjacent ice shelf (right bay). The figures show the ice-geometry at different stages of the simulation. The black line delineates the current calving fronts in panels e and f; the initial front of panels a and b is provided as a brown line for reference. Left panels show the minor strain-rate eigenvalue $\dot{\epsilon}_-$ (in units s^{-1}) which generally corresponds to the flow perpendicular to the main flow direction. Right panels provide the ice velocity as arrows on top of color-coded ice speed in different states of simulation (in panels d and f, anomalies to panel b are shown): Starting from an dynamically equilibrated geometry (top), the left ice–shelf is eliminated (centre). The bottom panels show a transient state 50 years after the event. The blue-dotted line marks the section along which the time series in Fig. 3 is evaluated.

simulations (Fig. 1), the speed of the ice-front retreat is unlikely to be modeled realistically with our model, especially because material properties of the ice and fracture physics is missing from the simulations.

4. Discussion and conclusions

The mechanism described here is qualitatively robust against changes in parameter and geometry and can indeed be clearly understood on physical grounds. The timing and exact position of the ice fronts in different stages, depends on the ice-softness, the inflow speed, the calving parameter $K_2^{\pm}$ and also on the resolution of the integration. Friction along the side margins generally stabilizes the ice–shelf flow by restraining the shear stresses within the ice. For the mechanism to be effective, the connecting channel between the ice shelves has to be wide enough to allow for the transfer of longitudinal stresses. The geometry of the embayment and hence the degree of confinement determines the flow pattern in the interior ice shelf and hence the curvature of the steady-state calving front position. The distribution of the inlet boundary velocity affects the occurrence and extent of divergent regions ($\dot{\epsilon}_- > 0$) in the interior ice shelf, which implies the possibility of a complete calving-front retreat.

The described mechanism has been studied in various simulations in simplified geometric situations and finds its realistic counterpart in the observed behavior of the Larsen A and B ice–shelf system prior to the complete disintegration in the year 2002. We tested the hypothesis that the disintegration of Larsen A induced the successive gradual calving of the Larsen B between the years 1995 and 2000. This reasoning is supported by the presented model simulation. However, the retreat of the calving front, though spontaneous, takes longer than observed. This is likely due to com-

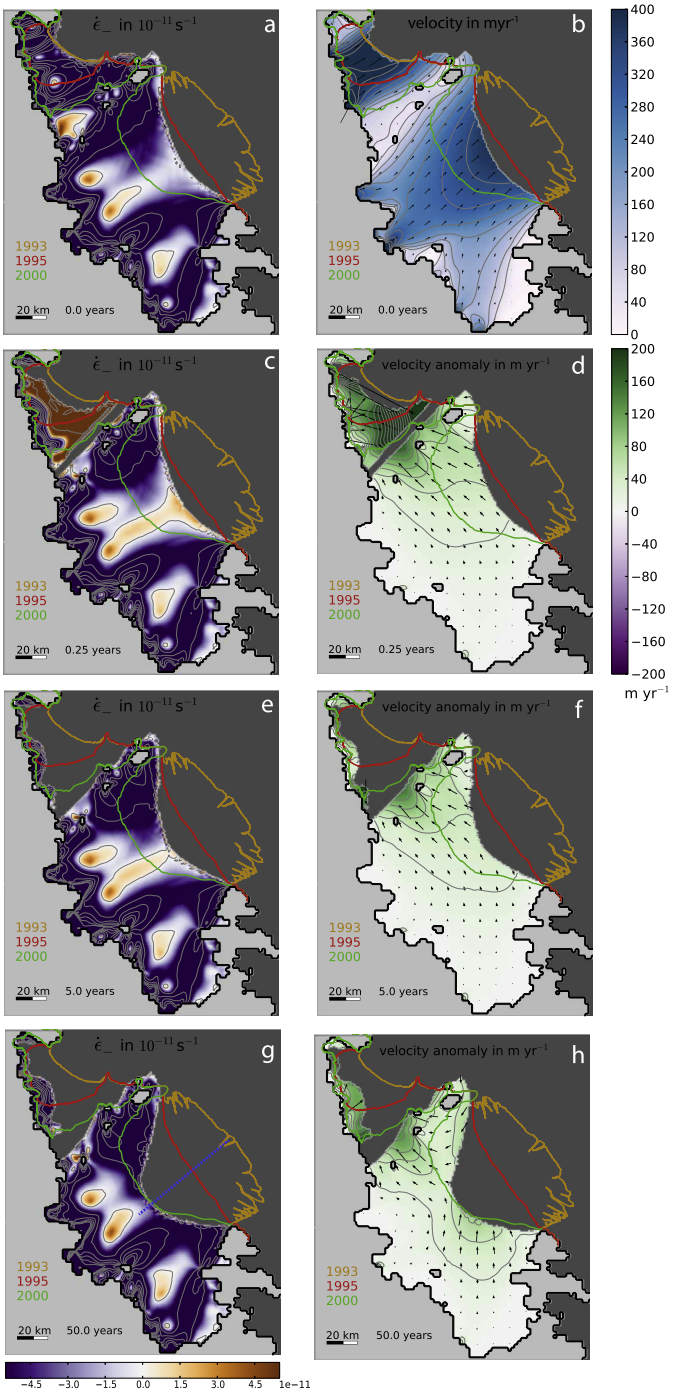

Fig. 2. Four states of the Larsen A and B Ice Shelf system chronologically from top to down as described in the text. As in Fig. 1 the minor spreading-rate eigenvalue $\dot{\epsilon}_-$ is shown on the left and ice shelf velocities (panel b) and their anomalies to the right. Following the disintegration of Larsen A the ice front of Larsen B shows a rapid retreat (compare Fig. 3) within the first five years. The steady state calving front position in the top panels as well as minimal front position 50 years after the disintegration of Larsen A in the bottom panels agree well with observed shapes of different dates of the late 1990s (colored contour lines are based on satellite data kindly provided by H. Rott). The blue-dotted line marks the section along which the time series in Fig. 3 is evaluated.

putational limitations associated with the spatial resolution, time step or unresolved inhomogeneities in the ice properties. It appears that two characteristic response times are involved: A short time scale with a spontaneous partial retreat within the first five years, where the calving rate directly responds to the changed strain-rate field. The longer time scale can be associated with a

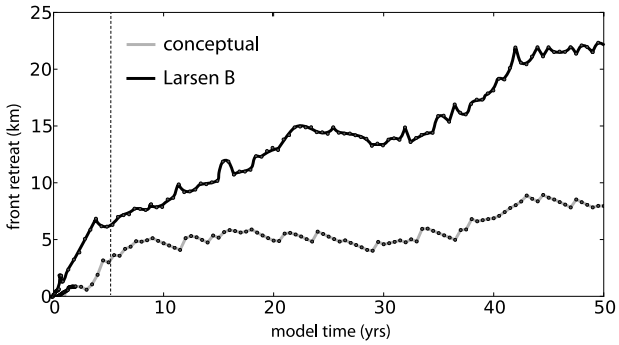

Fig. 3. Time series of the ice-front retreat for the conceptual set-up of Fig. 1 (light grey) and the Larsen Ice Shelf configuration of Fig. 2 (dark grey). In both cases a rapid initial retreat during the first 5 years (vertical dashed line) is followed by a more gradual retreat within a period of 50 years. The ice-front position was evaluated along the blue dashed lines in Figs. 1 and 2.

gradual retreat to a maximum retreat of the ice front after about 50 years (Fig. 3). This deceleration of the retreat is likely caused by the gradual dynamic adjustment of the ice–shelf flow and hence of the shelf-ice thickness to the abruptly changed stress conditions.

The mechanism could become relevant for a number of ice–shelf systems fringing the Antarctic Peninsula and East Antarctica, which might become more exposed to future warming than the larger more landlocked ice shelves Ross and Filchner-Ronne. In combination with a possible acceleration of ice flow across the grounding line due to reduced buttressing of a destabilized ice shelf, it might be relevant for future sea-level rise.

Acknowledgements

Model development at the University of Alaska, Fairbanks, USA was supported by the NASA grants NNX09AJ38C, NNX13AM16G, and NNX13AK27G. T.A. was funded by the German National Merit Foundation (Studienstiftung des deutschen Volkes).

Appendix A. Supplementary material

Supplementary material related to this article can be found online at http://dx.doi.org/10.1016/j.epsl.2014.02.034.

References

Albrecht, T., Martin, M., Haseloff, M., Winkelmann, R., Levermann, A., 2011. Parameterization for subgrid-scale motion of ice–shelf calving fronts. The Cryosphere 5, 35–44.

Alley, R.B., Horgan, H.J., Joughin, I., Cuffey, K.M., Dupont, T.K., Parizek, B.R., Anandakrishnan, S., Bassis, J., 2008. A simple law for ice–shelf calving. Science 322 (5906), 1344.

Bamber, J.L., Aspinall, W.P., 2013. An expert judgement assessment of future sea level rise from the ice sheets. Nat. Clim. Change 3 (4), 424–427.

Bueler, E., Brown, J., 2009. Shallow shelf approximation as a "sliding law" in a thermomechanically coupled ice sheet model. J. Geophys. Res. 114 (F3), F03008.

Cazenave, A., Llovel, W., 2010. Contemporary sea level rise. Ann. Rev. Mar. Sci. 2, 145–173.

Church, J., White, N., Konikow, L., Domingues, C., Cogley, J., Rignot, E., Gregory, J., van den Broeke, M., Monaghan, A., Velicogna, I., 2011. Revisiting the earth's sea-level and energy budgets from 1961 to 2008. Geophys. Res. Lett. 38 (18), L18601.

Cook, A.J., Vaughan, D.G., 2010. Overview of areal changes of the ice shelves on the Antarctic Peninsula over the past 50 years. The Cryosphere 4 (1), 77–98.

Courant, R., Friedrichs, K., Lewy, H., 1967. On the partial difference equations of mathematical physics. IBM J. Res. Dev. 11 (2), 215–234 [1928].

De Angelis, H., Skvarca, P., 2003. Glacier surge after ice shelf collapse. Science 299 (5612), 1560–1562.

Doake, C.S.M., 2001. Ice-shelf stability. In: Encyclopedia of Ocean Sciences, pp. 1282–1290.

Doake, C.S.M., Corr, H.F.J., Rott, H., Skvarca, P., Young, N.W., 1998. Breakup and conditions for stability of the Northern Larsen Ice Shelf, Antarctica. Nature 391 (6669), 778–780.

Dupont, T.K., Alley, R.B., 2005. Assessment of the importance of ice–shelf buttressing to ice-sheet flow. Geophys. Res. Lett. 32 (4), L04503.
Dupont, T.K., Alley, R.B., 2006. Role of small ice shelves in sea-level rise. Geophys. Res. Lett. 33 (9), L09503.
Ettema, J., van den Broeke, M.R., van Meijgaard, E., van de Berg, W.J., 2010. Climate of the Greenland ice sheet using a high-resolution climate model–Part 2: Near-surface climate and energy balance. The Cryosphere 4 (4), 529–544.
Fettweis, X., Franco, B., Tedesco, M., van Angelen, J.H., Lenaerts, J.T.M., van den Broeke, M.R., Gallée, H., 2013. Estimating the Greenland ice sheet surface mass balance contribution to future sea level rise using the regional atmospheric climate model MAR. The Cryosphere 7 (2), 469–489.
Fettweis, X., Tedesco, M., Broeke, M., Ettema, J., 2011. Melting trends over the Greenland ice sheet (1958–2009) from spaceborne microwave data and regional climate models. The Cryosphere 5 (2), 359–375.
Glasser, N.F., Scambos, T.A., 2008. A structural glaciological analysis of the 2002 Larsen B ice–shelf collapse. J. Glaciol. 54 (184), 3–16.
Gregory, J.M., White, N.J., Church, J.A., Bierkens, M.F.P., Box, J.E., van den Broeke, M.R., Cogley, J.G., Fettweis, X., Hanna, E., Huybrechts, P., Konikow, L.F., Leclercq, P.W., Marzeion, B., Oerlemans, J., Tamisiea, M.E., Wada, Y., Wake, L.M., van de Wal, R.S., 2012. Twentieth-century global-mean sea-level rise: is the whole greater than the sum of the parts? J. Climate, 4476–4499.
Hulbe, C.L., Scambos, T.A., Youngberg, T., Lamb, A.K., 2008. Patterns of glacier response to disintegration of the Larsen B ice shelf, Antarctic Peninsula. Glob. Planet. Change 63 (1), 1–8.
Joughin, I., Alley, R.B., 2011. Stability of the West Antarctic ice sheet in a warming world. Nat. Geosci. 4 (8), 506–513.
Le Brocq, A.M., Payne, A.J., Griggs, J., Nitsche, F., Shapiro, N., Van den Broeke, M., Vaughan, D., 2010. An improved Antarctic dataset for high resolution numerical ice sheet models (ALBMAP v1). http://doi.pangaea.de/10.1594/PANGAEA.734145.
Levermann, A., Albrecht, T., Winkelmann, R., Martin, M., Haseloff, M., Joughin, I., 2012. Kinematic first-order calving law implies potential for abrupt ice–shelf retreat. The Cryosphere 6, 273–286.
Levermann, A., Clark, P.U., Marzeion, B., Milne, G.A., Pollard, D., Radic, V., Robinson, A., 2013. The multi-millennial sea-level commitment of global warming. Proc. Natl. Acad. Sci. USA 110 (34), 13745–13750.
Ligtenberg, S.R.M., Van de Berg, W.J., Van den Broeke, M.R., Rae, J.G.L., Van Meijgaard, E., 2013. Future surface mass balance of the Antarctic ice sheet and its influence on sea level change, simulated by a regional atmospheric climate model. Clim. Dyn. 41, 867–884.
Lorbacher, K., Dengg, J., Böning, C.W., Biastoch, A., 2010. Regional Patterns of Sea Level Change Related to Interannual Variability and Multidecadal Trends in the Atlantic Meridional Overturning Circulation. J. Climate 23, 4243–4254.
MacAyeal, D.R., Scambos, T.A., Hulbe, C.L., Fahnestock, M.A., 2003. Catastrophic ice–shelf break-up by an ice–shelf-fragment-capsize mechanism. J. Glaciol. 49 (164), 22–36.
Payne, A.J., Holland, P.R., Shepherd, A.P., Rutt, I.C., Jenkins, A., Joughin, I., 2007. Numerical modeling of ocean–ice interactions under Pine Island Bay's ice shelf. J. Geophys. Res. 112 (C10), C10019.
Pfeffer, W.T., Harper, J.T., O'Neel, S., 2008. Kinematic constraints on glacier contributions to 21st-Century sea-level rise. Science 321 (5894), 1340.
Price, S.F., Payne, A.J., Howat, I.M., Smith, B.E., 2011. Committed sea-level rise for the next century from Greenland ice sheet dynamics during the past decade. Proc. Natl. Acad. Sci. USA 108 (22), 8978–8983.
Rack, W., Rott, H., 2004. Pattern of retreat and disintegration of the Larsen B ice shelf, Antarctic Peninsula. Ann. Glaciol. 39 (1), 505–510.
Rahmstorf, S., Cazenave, A., Church, J.A., Hansen, J.E., Keeling, R.F., Parker, D.E., Somerville, R.C., 2007. Recent climate observations compared to projections. Science 316 (5825), 709.
Rahmstorf, S., Foster, G., Cazenave, A., 2012. Comparing climate projections to observations up to 2011. Environ. Res. Lett. 7 (4), 044035.
Rignot, E., Casassa, G., Gogineni, P., Krabill, W., Rivera, A., Thomas, R., 2004. Accelerated ice discharge from the Antarctic Peninsula following the collapse of Larsen B ice shelf. Geophys. Res. Lett. 31, 18.
Rignot, E., Velicogna, I., van den Broeke, M.R., Monaghan, A., Lenaerts, J., 2011. Acceleration of the contribution of the Greenland and Antarctic ice sheets to sea level rise. Geophys. Res. Lett. 38 (5), L05503.
Rott, H., Müller, F., Nagler, T., Floricioiu, D., 2011. The imbalance of glaciers after disintegration of Larsen-B ice shelf, Antarctic Peninsula. The Cryosphere 5 (1), 125–134.
Rott, H., Rack, W., Nagler, T., 2008. Increased export of grounded ice after the collapse of northern Larsen Ice Shelf, Antarctic Peninsula, observed by Envisat ASAR. In: Geoscience and Remote Sensing Symposium, 2007. IGARSS 2007. IEEE International, pp. 1174–1176.
Scambos, T.A., Bohlander, J.A., Shuman, C.A., Skvarca, P., 2004. Glacier acceleration and thinning after ice shelf collapse in the Larsen B embayment, Antarctica. Geophys. Res. Lett. 31, L18402.
Shepherd, A., Ivins, E.R., Geruo, A., Barletta, V.R., Bentley, M.J., Bettadpur, S., Briggs, K.H., Bromwich, D.H., Forsberg, R., Galin, N., Horwath, M., Jacobs, S., Joughin, I., King, M.A., Lenaerts, J.T.M., Li, J., Ligtenberg, S.R.M., Luckman, A., Luthcke, S.B., McMillan, M., Meister, R., Milne, G., Mouginot, J., Muir, A., Nicolas, J.P., Paden, J., Payne, A.J., Pritchard, H., Rignot, E., Rott, H., Sorensen, L.S., Scambos, T.A., Scheuchl, B., Schrama, E.J.O., Smith, B., Sundal, A.V., van Angelen, J.H., van den Berg, W.J., van de Broeke, M.R., Vaughan, D.G., Velicogna, I., Wahr, J., Whitehouse, P.L., Wingham, D.J., Yi, D., Young, D., Zwally, H.J., 2012. A reconciled estimate of ice–sheet mass balance. Science 338 (6111), 1183–1189.
Solomon, S., 2007. Climate change 2007 – the physical science basis: Working group I contribution to the fourth assessment report of the IPCC. Tech. rep.
Stammer, D., Cazenave, A., Ponte, R.M., Tamisiea, M.E., 2013. Causes for contemporary regional sea level changes. Ann. Rev. Mar. Sci. 5 (1), 21–46.
Van den Broeke, M.R., Bamber, J., Lenaerts, J., Rignot, E., 2011. Ice sheets and sea level: Thinking outside the box. Surv. Geophys. 32 (4–5), 495–505.
Vieli, A., Payne, A.J., Du, Z., Shepherd, A., 2006. Numerical modelling and data assimilation of the Larsen B ice shelf, Antarctic Peninsula. Philos. Trans. R. Soc., Math. Phys. Eng. Sci. 364 (1844), 1815.
Winkelmann, R., Levermann, A., Martin, M.A., Frieler, K., 2012. Increased future ice discharge from Antarctica owing to higher snowfall. Nature 492 (7428), 239–242.
Winkelmann, R., Martin, M., Haseloff, M., Albrecht, T., Bueler, E., Khroulev, C., Levermann, A., 2011. The Potsdam Parallel Ice Sheet Model (PISM-PIK)–Part 1: Model description. The Cryosphere 5, 715–726.